ELSEVIER

Chemical Engineering Journal 138 (2008) 47–54

Chemical Engineering Journal

www.elsevier.com/locate/cej

Feasibility study of using carbon aerogel as particle electrodes for decoloration of RBRX dye solution in a three-dimensional electrode reactor

Xinbo Wu [a], Xiaoqing Yang [a], Dingcai Wu [a], Ruowen Fu [a,b,*]

[a] *Materials Science Institute, PCFM Laboratory, School of Chemistry and Chemical Engineering, Sun Yat-sen University, Guangzhou 510275, PR China*

[b] *Institute of Optoelectronic and Functional Composite Materials, PR China*

Received 25 October 2006; received in revised form 16 April 2007; accepted 16 May 2007

Abstract

The decoloration of RBRX from simulated dye wastewater in three-dimensional electrode reactor using granular carbon aerogels (CAs) as particle electrodes was experimentally investigated. Decolorization ratio can keep as high as 95% in the 100th run of treatment. Particular attention was paid to probe the function of the CAs through comparing the decolorization ratio of three-dimensional electrode reactor with single adsorption and two-dimensional electrode reactor. Conditional experiments were conducted to evaluate the effect of various parameters such as cell voltage, air flowrate, particle electrode dose, initial dye concentration and pH of the dye solution. The results showed that the decolorization rate increased with increasing cell voltage and particle electrode dose, but decreased with increasing the initial dye concentration. The decolorization rate increased firstly and then kept almost unchanged with the increase of airflow. In addition, the decolorization rate can be also controlled by the pH of the dye solution. The decolorization of RBRX was based on the break of the azo double bonds and the destruction of the other unsaturated bonds.

Keywords: Decoloration; Reactive dye; Carbon aerogel; Three-phase electrodes

1. Introduction

In recent years, the control and purification of water pollution has become an increasing concern. The release of dyes into the water constitutes only a small proportion of water pollution, but their presence in water, even at very low concentrations, is highly visible and undesirable [1]. Therefore, the decoloration of dye wastewater is one of indispensable processes in treatment of wastewater [2]. There are several physical, chemical and biological decolorization methods for treating dyeing wastewater. Amongst the numerous techniques of dye removal from an effluent, adsorption and biological treatment are two accepted and widely used methods. Adsorption is limited to the high cost of adsorbent and its regeneration. Biological treatment cannot be used in treating non-readily biodegradable pollutants such as most dyes [3]. Therefore, many investigators have been studying alternative oxidation methods, such as ozonation, photocatalytic oxidation, electrochemical oxidation, etc.

Electrochemistry offers several promising approaches that in many cases can be used to make "green" processes for the prevention of pollution problems [4]. The potential uses of electrochemistry for the purification of dye effluents have two approaches, one is electrochemical conversion of the dye molecules to other organic compounds which can be degraded easily using other methods [5], and the other is electrochemical combustion of the dye molecules to CO_2 and H_2O. However, both ways can be achieved using either direct electrolysis at the surface of electrode, or by generating a reactive intermediate product that attacks the pollutants in a subsequent step. Many related studies have been reported extensively [6–8]. In particular, the electrochemical technologies based on three-dimensional electrodes have been attracting much attention and interests. It has been recognized widely that the rate of conversion can be increased largely by the use of the three-dimensional electrode with extensive specific surface area in comparison to conventional two-dimensional electrodes [9–12]. In recent years, the research about the three-dimensional electrode deal with the organic pollutants focused on the design of the three-dimensional electrode reactor and the preparation of the particle electrode [13–15]. It is obvious that the property of particle

* Corresponding author at: Materials Science Institute, Sun Yat-sen University, Guangzhou 510275, PR China. Tel.: +86 20 84115112; fax: +86 20 84115112.
E-mail address: cesfrw@mail.sysu.edu.cn (R. Fu).

1385-8947/$ – see front matter © 2007 Elsevier B.V. All rights reserved.
doi:10.1016/j.cej.2007.05.027

electrodes has played the most important role in estimating performance of the total system [16]. The most commonly used particle electrodes is activated carbon that has been applied to the treating dye wastewater and has obtained the good effect [17–19]. It could be attributed to that activated carbon has good adsorbability and electricity activeness under the electrochemical condition [20].

Recently a noval mesoporous carbon material has been appeared: carbon aerogel (CA). CA has many excellent properties, such as low mass densities, continuous porosities, high surface areas, great mesopore volume and high electrical conductivity [21,22]. These characteristics are derived from their three-dimensional nano-network structures. In a previous study our research group has successfully obtained good results about improving techniques and reducing cost in the process of preparation of and CA [23,24]. In this paper, a soluble reactive azo dye, reactive brilliant red X-3B (RBRX) was selected as a model dyeing pollutant because reactive dyes are among the largest-group of colorants used in a variety of industries and they are stable with respect to biochemical oxidation. The main objectives of this paper were: (a) to determine the characterizations of CA prepared from sol–gel polymerization method with resorcinol (R), formaldehyde (F), surfactant (CTAB) and water; (b) to research the feasibility of using CA as particle electrodes for removal of RBRX dye from wastewater; (c) to determine the various parameters affecting the performance of the decoloration of RBRX, such as treating time, cell voltage, air flowrate, particle electrode dose, initial dye concentration and pH of dye solution.

2. Materials and methods

2.1. Dye material

The textile dye, RBRX was purchased from Shanghai Dyestuffs Co., Ltd. of China, and it was used as received without further purification. The molecular structure of RBRX is shown in Fig. 1.

2.2. Preparation and characteristic of particle electrodes

About 165 g resorcinol (R), 207.9 mL formaldehyde (F) and appropriate catalyst (CTAB) were mixed with 240.9 mL water according to predetermined recipes, and then transferred into a 600 mL glass vial. The vial was sealed and then put into a water bath at 70 °C to cure for 1 day and then cure for 5 days at 85 °C. After curing, the sample were directly dried in air at room temperature for 2 days at first, and further dried under an infrared lamp for 24 h, and finally dried in an oven at 105 °C at ambient pressure for 3 h. Subsequently, the dried sample was heated to 900 °C with a heating rate of 5 °C/min and kept at this carbonization temperature for 3 h in flowing N_2 (800 mL/min).

The BET surface area (S_{BET}), micropore size distribution, the micropore volume (V_{mic}), micropore surface area (S_{mic}), mesopore size distribution and mesopore volume (V_{mes}) of the samples were analyzed by Micromeritics ASAP 2010 instrument. The scanning electron microscopy of samples were mounted on a sample holder, coated with Au alloy, and then examined by JSM-6330F equipment. CAs powder was dispersed with ethanol onto a copper grid for transmission electron microscopy by JEM-2010HR equipment. X-ray diffraction (XRD) patterns were collected using a diffractometer equipped with a Cu Kα source by D/MAX 2200 VPC equipment.

2.3. Experimental set-up of three-phase three-dimensional electrode reactor

The experimental set-up is shown schematically in Fig. 2. A rectangular reactor support was made of plastic. The main anode and cathode, situated 10.0 cm apart from each other, were made of graphite and stainless steel plates, respectively. Forty grams of CAs pellets (5–10 mesh, from which the fraction with of 0.4–0.2 cm diameter was selected) was packed between the two electrodes to form a three-dimensional electrode (working electrode) with a bed height of approximately 6 cm. The volume of the three-dimensional electrodes is 10.0 cm × 2.3 cm × 6.0 cm. Compressed air was sparged into the three-dimensional electrodes system by a micropore pipe from the bottom of the reactor. The electric power was supplied with regulated dc power supply, TPR640, China.

2.4. Experimental method

A simulated wastewater containing RBRX was diluted to a concentration of 800 mg/L with ultra-pure water. No electrolyte was added and the pH value was not adjusted unless otherwise

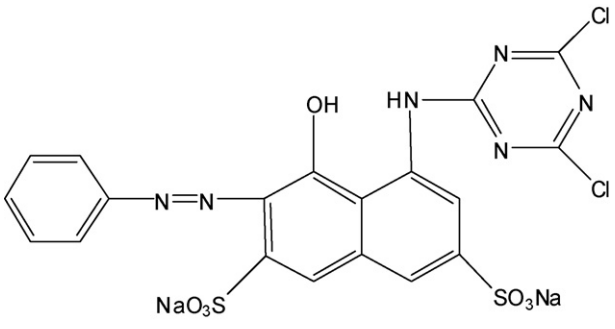

Fig. 1. Structure of RBRX (chemical formula: $C_{19}H_{10}O_7N_6Cl_2S_2Na_2$; molecular weight: 615).

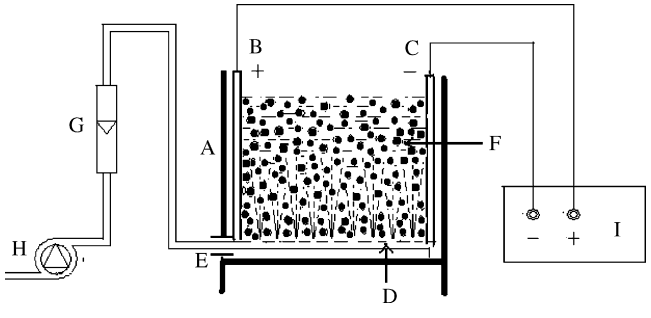

Fig. 2. Experimental set-up: (A) supporter; (B) main anode (graphite plate); (C) main cathode (stainless steel plate); (D) micropore pipe; (E) compressed air; (F) CAs particle electrodes; (G) airflow meter; (H) controlled volume pump; (I) dc stabilized voltage supply.

stated. A total of 100 mL of the wastewater was fed into the reactor prior to each run. The reaction was started when the dc electrical power and compressed air supply were switched on. The solution obtained was filtered to remove any traces of CA and then was analyzed.

In order to probe the behavior of the carbon aerogel electrodes for decolorization ratio and COD removal efficiency in the process of continuous use, every carbon aerogel electrodes was repeatedly used 100 times (30 min per time) under same experimental conditions. When a run stopped, all solutions were taken out from reactor and assessed with decolorization ratio and COD removal.

In conditional experiments, the 2 mL sample was carefully withdrawn from the reactor at predetermined time intervals using a digital micropipette and was assessed mainly with decolorization ratio. The effect of pH was studied by adjusting the pH of dye solutions using dilute HCl and NaOH solutions.

Decolorization efficiencies were measured with spectrophotometer method [17]. All RBRX solutions were analyzed by a UV/VIS spectrophotometer (756, China) at a maximum wavelength of 538 nm. The final concentration of the solution was then determined from the calibration curve. COD was measured with potassium dichromate after the filtered sample was digested with a WMX COD microwave digestion system (Huanhai Engineering Company of Shantou).

3. Results and discussion

3.1. Characteristic of particle electrode

According to the N_2 adsorption–desorption isotherm of the sample, the specific surface area, specific pore volume and pore size distribution of the sample were obtained and the results were shown in Table 1 and Fig. 3. It can be discovered that the CA has a wide pore size distribution. As we know, the pores, including mesopores and macropores in CAs are attributed to the interval gap between chains of interconnected particles [23]. The data listed in Table 1 reveal that the CA has high mesopore volume and high BET surface areas. It has several narrow micropore diameters (range from 0.6 to 1.1 nm) and a narrow mesopore diameter (range from 10 to 14 nm). Fig. 4 shows the X-ray diffraction pattern of CA. The broad peak at $2\theta = 23^\circ$ indicates that the CA prepared is a graphite-like micro-crystal carbon, similar to that of activated carbons and activated carbon fibers [23]. Fig. 5 shows the TEM and SEM photographs of CA samples. TEM observations indicated that CAs have a three-dimensional network. The solid phase is composed of interconnected carbon nano-particles with a size range from 20 to 30 nm and the nano-particles are not very round in shape. There are an abundant number of nanopores with different sizes among the interconnected carbon nano-particles. From the SEM in Fig. 5, we can see that carbon nano-particles are interconnected into the nano-scale of the aggregates like bunches of grapes, which are connected into a bulk network. There are many mesopores and macropores among the carbon nano-particles and nano-scale aggregates. These results are consistent with the TEM images.

Table 1
Textual characteristics of the representative samples in the study

Sample	CA-125
S_{BET} ($m^2\,g^{-1}$)	582.7
S_{micro} ($m^2\,g^{-1}$)	312.8
S_{BJH} ($m^2\,g^{-1}$)	269.9
V_{micro} ($cm^3\,g^{-1}$)	0.145
V_{BJH} ($cm^3\,g^{-1}$)	1.150
A.P.D_{BJH} (Å)	152.3

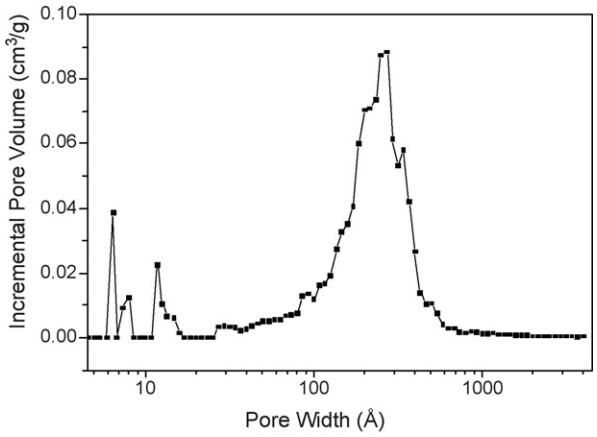

Fig. 3. Pore size distributions of the CA.

The above discussion clearly shows that CA we prepared is a porous, high surface area, graphite-like micro-crystal carbon material with a three-dimensional network structure. Considering those characteristics of CA, it is natural to associate them with the particle electrodes in three-dimensional electrode.

3.2. The function of CAs

In order to probe the behavior and effect of the CA particle electrodes for decolorization ratio in the process of dye decoloration, we have compared the decolorization ratio of pure adsorption of CAs, two-dimensional electrode system and three-dimensional electrode with CAs as particle electrodes under the same condition. Considering CA has a good adsorbability,

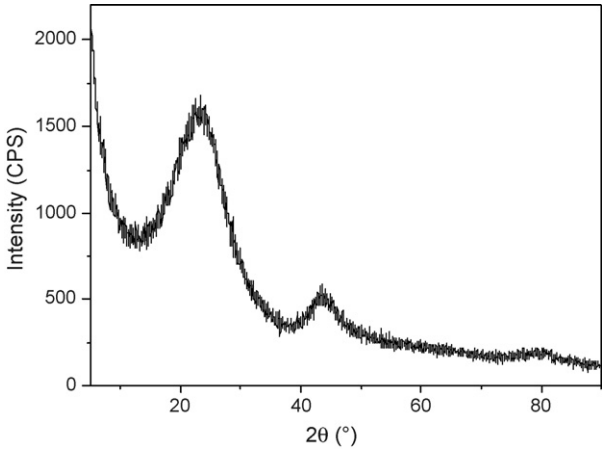

Fig. 4. XRD pattern for the CA.

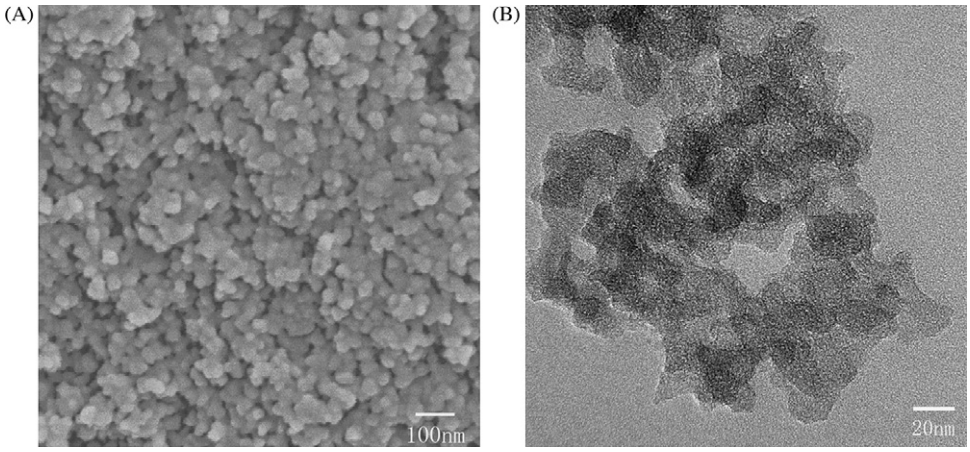

Fig. 5. SEM and TEM photographs of CA sample: (A) SEM and (B) TEM.

every process was repeated 100 times under various conditions. *N* was used to represent the number of repeated runs. The experimental results were assessed by decolorization ratio of RBRX. Decolorization ratio under various treatment conditions were presented in Fig. 6. In Fig. 6, curve a showed that the decolorization ratio under the condition of single adsorption process, curve b expressed that the decolorization ratio under the condition of single two-dimensional electrode system and curve c showed that the decolorization ratio under the condition of three-dimensional electrode system. It can be observed that the decolorization ratios for adsorption, two-dimensional electrode reactor and three-dimensional electrode reactor exhibit obvious difference from Fig. 6, and the decolorization ratio of three-dimensional electrode reactor is much higher than others. The difference of decolorization ratios indicated that the three-dimensional electrode system is more efficient than the adsorption process and two-dimensional electrode system, and even greater than the sum of the two processes. The result explains that good decolorization rate should be attributed to the combination of adsorption and electrochemical oxidation. At the same time, CA has an effect on the destruction of chromophore of dyestuff.

3.3. Effect of cell voltage

The effects of applied voltages on the decolorization ratio were conducted and the results were shown in Fig. 7. It was obviously found that decolorization ratio in the electrochemical processes increased with the increase of the cell voltage from 10 to 30 V. When the applied voltage was 10, 20 and 30 V, the decolorization ratio was 60, 82 and 97%, respectively, on treatment time for 10 min. We could conclude that with the increase of electric field strength, the electrical charges on the polarized CA particles would increase accordingly. These particles would be more effective electrically in participation of the dye decoloration or mineralization. At the same, we could see that decolorization ratio in the electrochemical processes increased sharply with the increase of the treatment time. Furthermore, the difference in degree of increase for their decolorization ratio with applied voltage was also dependent on treatment time.

3.4. Effect of airflow

When the reaction started, the compressed air was uniformly sparged into the reactor by a micropore pipe. Fig. 8 presents the

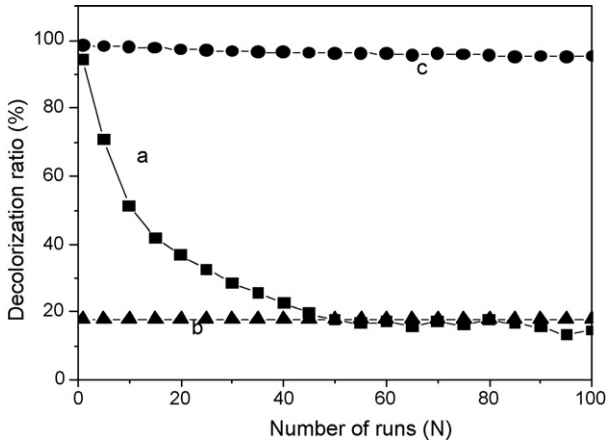

Fig. 6. Decolorization ratio in various conditions: (a) single adsorption process; (b) single two-dimensional electrode system; (c) three-dimensional electrode system.

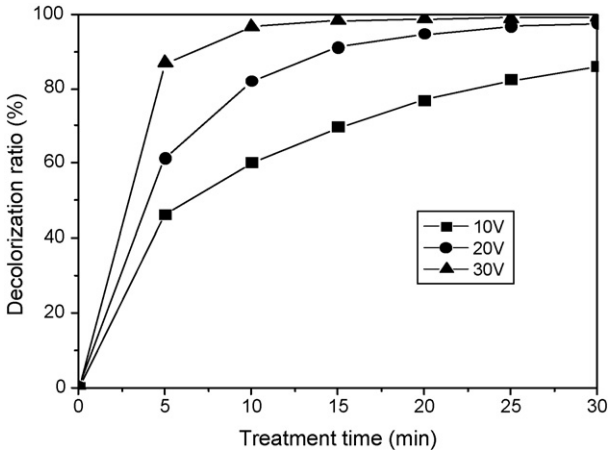

Fig. 7. Effect of the voltage on the decolorization ratio (operating conditions: air flowrate = 0.4 L min^{-1}, treatment time = 30.0 min).

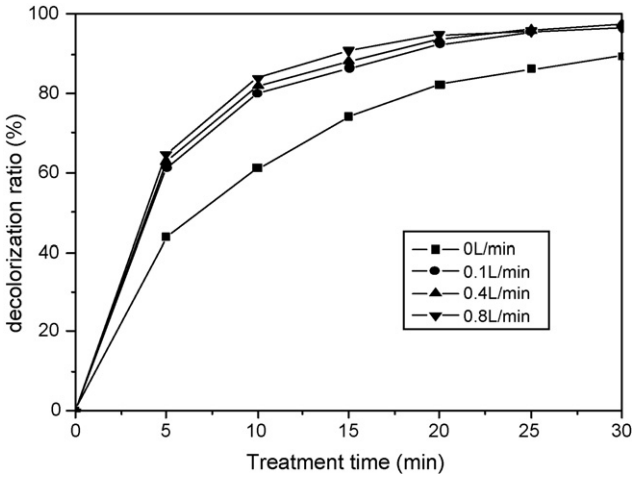

Fig. 8. Effect of air flowrate on the decolorization ratio (operating conditions: cell voltage = 20 V, treatment time = 30.0 min).

decolorization ratio versus air flowrate. As shown in Fig. 8, the decolorization ratio would increase with air flowrate. Namely, a greater air flowrate corresponds to a higher decolorization ratio. When the applied air flowrate was 0.0, 0.1, 0.4 and 0.8 L min^{-1}, the decolorization ratio was 61, 80, 82 and 84%, respectively, on treatment time for 10 min. We could conclude that the sparged compressed air plays an important role in the decolorization of RBRX. In fact, the sparged air in this system serves two purposes [18]. One of the functions of sparged air is to agitate in order to speed mass transfer. Another was to supply the essential oxygen for electrochemical reactions. Some authors have reported that the oxygen can be changed into a stronger oxidizing agent, H_2O_2, on activated carbon electrodes by the two-electron reduction of oxygen [25,26]. Thus, the three-phase three-dimensional electrodes could simultaneously make use of anodic oxidation and cathodic electrogenerated H_2O_2 to degrade organic pollutants. We also found from Fig. 8, when the air flowrate exceed 0.1 L min^{-1}, the decolorization ratio would increase slowly. It could be ascribed that the quantity of oxygen was almost saturated in the solution when the air flowrate exceed 0.1 L min^{-1}. The increasing oxygen just played the role to stir the solution, so the decolorization ratio gradually approaching the limiting value. Hence, it is feasible to keep a suitable air flowrate in the treatment [27].

3.5. Effect of particle electrode dose

The investigation of the effect of particle electrode dose on decolorization ratio of CA was shown in Fig. 9. When increasing the dose of particle electrodes, the decolorization ratio would increase accordingly. When 13.3 g of CA was added, the decolorization ratio was only 46 and 79% on treatment time for 10 and 30 min, respectively. When CA dose increased to 26.6 or 40.0 g, the decolorization ratio increased to 71 or 82% on treatment time for 10 min, and 96 or 98% on treatment time for 30 min, respectively. The increase of decolorization ratio was attributed to the increase of surface area of electrodes which leads to the increase of the reaction degree of RBRX on the surface of electrodes.

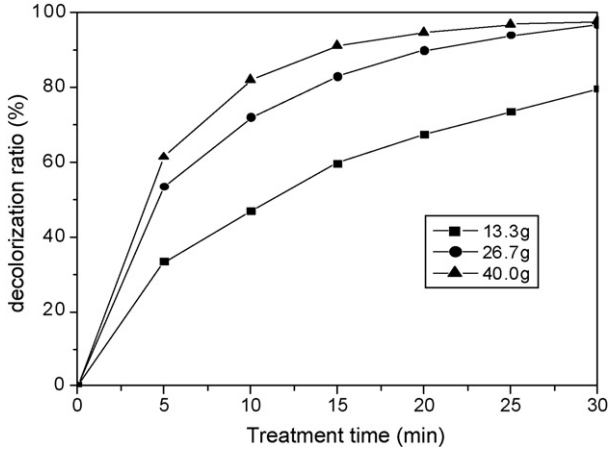

Fig. 9. Effect of particle electrode on the decolorization ratio (operating conditions: cell voltage = 20 V, treatment time = 30.0 min, air flowrate = 0.4 L min^{-1}).

3.6. Effect of initial concentration of dye

The investigation of the effect of RBRX initial concentrations on the decolorization ratio was carried out in the range of 400–1200 mg L^{-1} RBRX aqueous solution at 30 °C. Fig. 10 shows the decolorization ratio of RBRX treated for 30 min at different initial concentrations. It was observed that the decolorization ratio decreased with the increase of the initial concentration of RBRX when the dye concentration exceeded 800 mg L^{-1}, but the change in initial dye concentration had no effect on the dye removal below 800 mg L^{-1} after treatment for 30 min. This could be explained by surmising that when the dye concentration exceeded 800 mg L^{-1}, removal of the dye was incomplete and required a higher current density.

3.7. Effect of pH

The solution pH affected the structural stability of RBRX. Therefore, the pH value of the dye solution might affect the decolorization ratio of RBRX solution. The initial pH values of the dye solution were set at 2.8, 5.1 (original) and 9.6, respec-

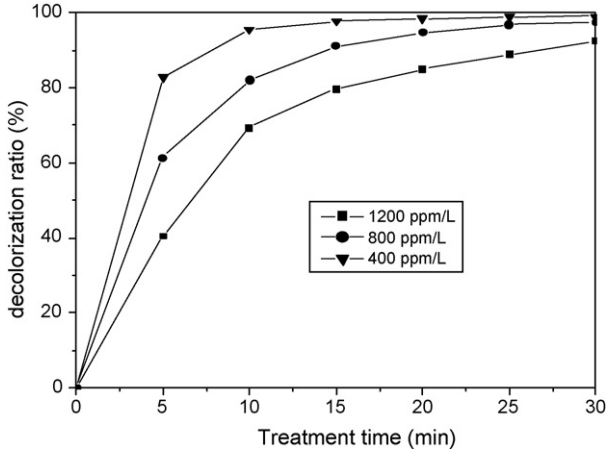

Fig. 10. Effect of initial dye concentration on the decolorization ratio (operating conditions: cell voltage = 20 V, treatment time = 30.0 min, air flowrate = 0.4 L min^{-1}).

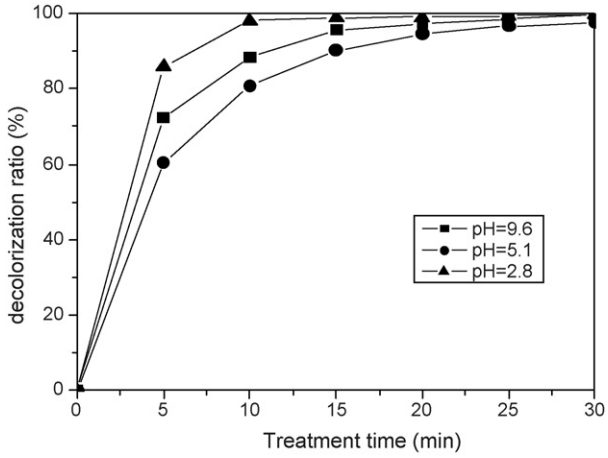

Fig. 11. Effect of pH on the decolorization ratio (operating conditions: cell voltage = 20 V, treatment time = 30.0 min, air flowrate = 0.4 L min^{-1}).

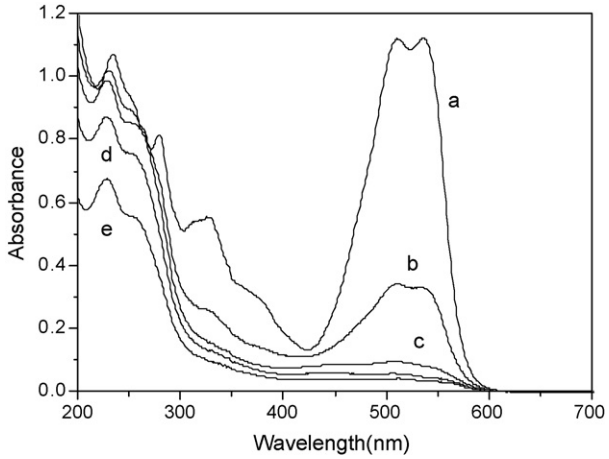

Fig. 12. Absorption spectra of RBRX with 15-fold dilution at various treating time: (a) 0 min; (b) 5 min; (c) 10 min; (d) 15 min; (e) 30 min.

tively, to determine its effect on decolorization ratio of RBRX. The results are shown in Fig. 11. It could be seen from Fig. 11 that when the pH of the dye solution was changed, the decolorization rate changed accordingly. For example, with respect to initial pH 2.8, 5.1 and 9.6, the decolorization ratio changed to 98.1, 81.0 and 88.4% on treatment time for 10 min, respectively. Additional experiments showed that the order on adsorption velocity of CAs for RBRX is as follows: pH 2.8 > pH 9.6 > pH 5.1. Therefore, the change of decolorization ratio with pH could be explained from the following two facts: one was the change of the adsorbability, and the other was that the electrochemical reaction of decoloration more easily occurred in acidic and basic solutions.

3.8. Decolorization kinetic of RBRX

In this study, pseudo-first-order kinetic was introduced to evaluate the influence of affected factors. The linearised form of pseudo-first-order kinetic can be written as follows:

$$\log(1 - A) = a + bt$$

where A is the decolorization ratio and t is the treating time. First-order decolorization rate constants were obtained from the slope of the linearised data and were shown in Table 2. From the data presented, it was seen that the correlation coefficients were higher than 0.9. Thus, the pseudo-first-order kinetic equation is satisfactory with the experimental data, indicating the validity of this equation. The kinetic rate constant data and half-life time reveal that RBRX is easily decolorizated in three-phase three-dimensional electrode reactor using carbon aerogel as particle electrodes. We can seen that the decolorization of RBRX is relatively easy when increasing voltage, air flow rate, weight of particle electrodes or decreasing initial dye concentration. Moreover, the values of kinetic rate constant increases in acid or base medium.

3.9. Investigation of decolorization process

The UV spectra of RBRX at various treatment times were presented in Fig. 12. It could be observed from Fig. 12 that the absorption peaks for electrochemical oxidation or degradation decreased obviously with prolonging the treatment time. At 538 nm, the absorption of the curve e is only 2.9% of curve a. These changes of UV spectra indicated that the decoloration of RBRX was efficient with the electrochemical process. It is well known that different structure units and groups in the dye molecules have different absorbance peaks. The main conju-

Table 2
Kinetics parameters of RBRX degradation in various conditions

Voltage (V)	Air flowrate (L min^{-1})	Electrode weight (g)	pH	Concentration (ppm/L)	Regression coefficiency	Kinetic constant (min^{-1})	Half-life (min)
10	0.4	40		800	0.988	0.026	8.0
20	0	40		800	0.992	0.032	7.3
20	0.1	40		800	0.988	0.048	3.6
20	0.4	13.3		800	0.995	0.022	11.9
20	0.4	26.6		800	0.998	0.047	5.3
20	0.4	40	2.8	800	0.967	0.076	0.7
20	0.4	40		800	0.988	0.054	3.3
20	0.4	40		400	0.927	0.063	1.8
20	0.4	40		1200	0.989	0.037	6.3
20	0.4	40	9.6	800	0.984	0.066	1.7
20	0.8	40		800	0.985	0.055	2.7
30	0.4	40		800	0.933	0.068	2.2

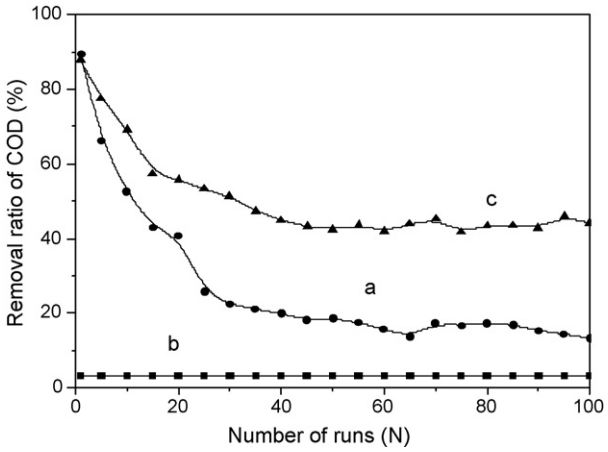

Fig. 13. COD removal efficiency in various conditions: (a) single adsorption process; (b) single two-dimensional electrode system; (c) three-dimensional electrode system.

gated structure of RBRX includes azo linkage, benzene ring and naphthalene ring. The chromophore containing azo linkage has absorption in the visible region, while benzene ring and naphthalene ring in the UV region, and naphthalene ring absorption wavelength is higher than that of benzene ring. From Fig. 12, we can see that RBRX has an absorption peak at 538 nm in the visible region is related to azo double bonds. In the near UV region, RBRX has three absorbance peaks at 232, 280 and 324 nm are, respectively, attributed to benzene ring and naphthalene ring. When compared the UV spectra of treated dye solution with original dye solution, it was shown that the decoloration resulted from the destruction of the conjugated azo double bonds and the other unsaturated system of the dyestuff. We could also see clearly that the destruction of the conjugated azo double bonds occur firstly, then the destruction of the other unsaturated system of the dyestuff take place along with progress of the electrochemistry reaction. Moreover, the destruction of the other unsaturated system of the dyestuff has not completed after treatment for 30 min. These results are consistent with the analysis of COD removal rate. The rate of COD removal under various treatment conditions was presented in Fig. 13. It can be observed from Fig. 13 that the rates of COD removal for single adsorption, single two-dimensional electrode reactor and three-dimensional electrode reactor different with the decolorization ratio (see Fig. 6) obviously increased in order. The rate of COD removal was lower than decolorization ratio with three-dimensional electrode systems, and this indicated that RBRX degraded incompletely under our experimental conditions, and part of RBRX was changed into intermediary products.

4. Conclusions

The performance of the decoloration of the RBRX dye wastewater was experimentally investigated using three-phase three-dimensional electrode reactor with granular CA as particle electrodes. The decolorization ratio can still reach as high as 95% after more than 100th treatment run. The study has proved the feasibility of using CA as the particle electrodes for the removal of RBRX dye from wastewater. Experiment results showed that decolorization ratio with three-dimensional electrode reactor was much higher than single adsorption and single two-dimensional electrode reactor. The results affirmed CA prepared from sol–gel polymerization method with resorcinol (R), formaldehyde (F), surfactant (CTAB) and water has an effect on the removal color of RBRX. Various parameters affecting decolorization ratio of RBRX are as follows: the decolorizing rate increases with the increase of treating time, cell voltage and particle electrode dose but decreases with initial dye concentration. The decolorizing rate increased firstly and then almost unchanged with the increase of airflow. The decolorizing rate increased when pH was changed from 5.1 to 2.8 or 9.6. The decoloration of RBRX was found to be the azo double bonds and the destruction of unsaturated system.

Acknowledgements

This research was supported by the Project of NNSFC (50472029, 50632040), the Foundation of SRFDP, and the Scientific Foundation of Guangdong (2004A30404001).

References

[1] T. Robinson, G. Mullan, R. Marchant, P. Nigam, Remediation of dyes in textile effluent: a critical review on current treatment technologies with a proposed alternative, Bioresour. Technol. 77 (2001) 247–255.
[2] I. Arslan, I. Akmehmet Balcioglu, Degradation of commercial reactive dyestuffs by heterogeneous and homogenous advanced oxidation processes: a comparative study, Dyes Pigments 43 (1999) 95–108.
[3] L. Fan, F. Yang, W. Yang, Performance of the decoloration of an azo dye with bipolar packed bed cell, Sep. Purif. Technol. 34 (2004) 89–96.
[4] K. Juttner, U. Galla, H. Schmieder, Electrochemical approaches to environmental problems in the process industry, Electrochim. Acta 45 (2000) 2575–2594.
[5] S.M. McClung, A.T. Lemley, Electrochemical treatment and HPLC analysis of wastewater containing acid dyes, Text. Chem. Color. 26 (1994) 17–22.
[6] J. Jia, J. Yang, J. Liao, W. Wang, Z. Wang, Treatment of dyeing wastewater with ACF electrodes, Water Res. 33 (1999) 881–884.
[7] N. Mohan, N. Balasubramanian, In situ electrocatalytic oxidation of acid violet 12 dye effluent, J. Hazard. Mater. B 136 (2006) 239–243.
[8] A. Sakalis, K. Fytianos, U. Nickel, A. Voulgaropoulos, A comparative study of platinised titanium and niobe/synthetic diamond as anodes in the electrochemical treatment of textile wastewater, Chem. Eng. J. 119 (2006) 127–133.
[9] C.J. Brown, D. Pletcher, F.C. Walsh, J.K. Hammond, D. Robinson, Studies of three-dimensional electrodes in the FM01-LC laboratory electrolyser, J. Appl. Electrochem. 24 (1994) 95–106.
[10] P. Tissot, M. Fragniere, Anodic oxidation of cyanide on a reticulated three-dimensional electrodes, J. Appl. Electrochem. 24 (1994) 509–512.
[11] C.L.K. Tennakoon, R.C. Bhardwaj, J.O. Bockris, Electrochemical treatment of human wastes in a packed bed reactor, J. Appl. Electrochem. 26 (1996) 18–29.
[12] J.O. Bockris, J. Kim, Effect of contact resistance between particles on the current distribution in a packed bed electrode, J. Appl. Electrochem. 27 (1997) 890–901.
[13] W. Kong, B. Wang, H. Ma, L. Gu, Electrochemical treatment of anionic surfactants in synthetic wastewater with three-dimensional electrodes, J. Hazard. Mater. 137 (2006) 1532–1537.
[14] A.M. Polcaro, S. Palmas, F. Renoldi, M. Mascia, Three-dimensional electrodes for the electrochemical combustion of organic pollutants, Electrochim. Acta 46 (2000) 389–394.

[15] C. He, Y. Xiong, D. Shu, X. Zhu, Performances of three-phase three-dimensional electrode reactor and its application to the degradation of aniline, Chemistrymag. Org. 4 (2002) 56–61.
[16] M. Zhou, L. Lei, The role of activated carbon on the removal of *p*-nitro phenol in an integrated three-phase electrochemical reactor, Chemosphere 65 (2006) 1197–1203.
[17] T. An, X. Zhu, Y. Xiong, Feasibility study of photoelectrochemical degradation of methylene blue with three-dimensional electrode-photocatalytic reactor, Chemosphere 46 (2002) 897–903.
[18] Y. Xiong, P.J. Strunk, H. Xia, X. Zhu, H. Karlsson, Treatment of dye wastewater containing acid orange II using a cell with three-phase three-dimensional electrode, Water Res. 35 (2001) 4226–4230.
[19] T. An, C. He, X. Zhu, Electrically assisted photocatalytic degradation of direct sky blue aqueous solution with three-dimensional electrodes, Chin. J. Catal. 22 (2) (2001) 193–197 (in Chinese).
[20] Y. Xiong, C. He, H.T. Karlsson, X. Zhu, Performance of three-phase three-dimensional electrode reactor for the reduction of COD in simulated wastewater-containing phenol, Chemosphere 50 (2003) 131–136.
[21] R.W. Pekala, Organic aerogels from the polycondensation of resorcinol with formaldehyde, J. Mater. Sci. 24 (1989) 3221–3227.
[22] M.S. Dresselhaus, Future directions in carbon science, Annu. Rev. Mater. Sci. 27 (1997) 1–34.
[23] D. Wu, R. Fu, M.S. Dresselhaus, G. Dresselhaus, Fabrication and nano-structure control of carbon aerogels via a microemulsion-templated sol–gel polymerization method, Carbon 44 (2006) 675–681.
[24] D. Wu, R. Fu, S. Zhang, M.S. Dresselhaus, G. Dresselhaus, Preparation of low-density carbon aerogels by ambient pressure drying, Carbon 42 (2004) 2033–2039.
[25] A. Alverez-Gallbergos, D. Pletcher, The removal of low level organics via hydrogen peroxide formed in aveticulated vitreous carbon cathode cell. Part2. The removal of phenols and related compounds from aqueous effluents, Electrochim. Acta 44 (1999) 2483–2492.
[26] P.C. Foller, R.T. Bombard, Processes for the production of mixtures of caustic soda and hydrogen peroxide via the reduction of oxygen, J. Appl. Electrochem. 25 (1995) 613–627.
[27] Y. Xiong, H.T. Karlsson, An experimental investigation of chemical oxygen demand removal from the wastewater containing oxalic acid using three-phase three-dimensional electrode reactor, Adv. Environ. Res. 7 (2002) 139–145.